



No. 110 – December 2002

## Installation and Commissioning of FLAMES, the VLT Multifibre Facility

L. PASQUINI<sup>1</sup>, G. AVILA<sup>1</sup>, A. BLECHA<sup>2</sup>, C. CACCIARI<sup>3</sup>, V. CAYATTE<sup>4</sup>, M. COLLESS<sup>5</sup>, F. DAMIANI<sup>6</sup>, R. DE PROPRIIS<sup>5</sup>, H. DEKKER<sup>1</sup>, P. DI MARCANTONIO<sup>7</sup>, T. FARRELL<sup>8</sup>, P. GILLINGHAM<sup>8</sup>, I. GUINOARD<sup>4</sup>, F. HAMMER<sup>4</sup>, A. KAUFER<sup>9</sup>, V. HILL<sup>4</sup>, M. MARTEAUD<sup>4</sup>, A. MODIGLIANI<sup>1</sup>, G. MULAS<sup>10</sup>, P. NORTH<sup>2</sup>, D. POPOVIC<sup>8</sup>, E. ROSSETTI<sup>3</sup>, F. ROYER<sup>2</sup>, P. SANTIN<sup>7</sup>, R. SCHMUTZER<sup>9</sup>, G. SIMOND<sup>2</sup>, P. VOLA<sup>4</sup>, L. WALLER<sup>8</sup>, M. ZOCCALI<sup>1</sup>

<sup>1</sup>European Southern Observatory, Garching, Germany; <sup>2</sup>Observatoire de Genève, Sauverny, Suisse;

<sup>3</sup>INAF-OABO, Bologna, Italy; <sup>4</sup>Observatoire de Paris-Meudon, Meudon, France;

<sup>5</sup>Research School of Astronomy and Astrophysics, Australian National University, Canberra, Australia;

<sup>6</sup>INAF-OAPa, Palermo, Italy; <sup>7</sup>INAF-OATs, Trieste, Italy; <sup>8</sup>Anglo Australian Observatory, Sydney, Australia;

<sup>9</sup>European Southern Observatory, Chile; <sup>10</sup>INAF-OACa, Capoterra, Cagliari, Italy

### Introduction

FLAMES (Fibre Large Array Multi Element Spectrograph) is the VLT Fibre Facility, installed and commissioned at the Nasmyth A focus of UT2 (Kueyen Telescope). FLAMES was built and assembled in about four years through an international collaboration between ten institutes in six countries and three continents. It had first light with the fibre link to the red arm of UVES on April 1, and with the GIRAFFE spectrograph on



Figure 1: The fibre positioner and GIRAFFE as seen during the GIRAFFE integration on the Nasmyth platform. The positioner is looking towards the Nasmyth Focus, where the corrector is placed (only the corrector support is visible). GIRAFFE is open, and all the optomechanics components are visible. The picture was taken when the OzPoz enclosure had not yet been installed.

Table 1. Observational capabilities of FLAMES.

Spectrograph	Mode	Nr. Objects	Aperture	R	Coverage (nm)
UVES8 Red Arm (with sky)		8	1	47000	200, 400
UVES7 Red Arm (with sky)	Simult. Calibration	7	1	47000	200
GIRAFFE	MEDUSA	132 (with sky)	1.2	20500*	$\lambda/22^*$
GIRAFFE	MEDUSA	132 (with sky)	1.2	7000*	$\lambda/7^*$
GIRAFFE	IFU	15 (+15 sky)	$2 \times 3$	33000*	$\lambda/22^*$
GIRAFFE	IFU	15 (+15 sky)	$2 \times 3$	11000*	$\lambda/7^*$
GIRAFFE	ARGUS	1	11.5 $\times$ 7.3 Or 6.6 $\times$ 4.2	33000*	$\lambda/22^*$
GIRAFFE	ARGUS	1	11.5 $\times$ 7.3 Or 6.6 $\times$ 4.2	11000*	$\lambda/7^*$

\*The GIRAFFE resolving power (R) and wavelength coverage given here are only average values. They will vary for the different set-ups by  $\pm \sim 20\%$ . Aperture is in arcseconds.

July 3. We report here on the complex process of integration and commissioning, and we compare the expected and observed astronomical requirements.

## Overview

FLAMES is the multi-object, intermediate and high-resolution fibre facility of the VLT. Mounted at the Nasmyth A platform of UT2 it offers a large corrected field of view (25 arcmin diameter) and it consists of several components, developed by several consortia (Australis (AAO/ANU/UNSW), Paris-Meudon (OPM), Geneva and Lausanne (OGL), Bologna, Cagliari, Palermo and Trieste (ITAL Consortium)) and ESO:

- An optical *Corrector*, providing excellent image quality and telecentricity over the full field of view of 25 arcmin diameter (developed at ESO).

- A *Fibre Positioner* hosting two plates. While one plate is observing, the other one is positioning the fibres for the subsequent observations, therefore limiting the dead time between observations (developed at AAO).

- A link to the *UVES* spectrograph (Red Arm) via eight single object fibres/plate (developed at OPM in collaboration with ESO).

- A high and intermediate resolution optical spectrograph, *GIRAFFE* (developed at OPM and ESO).

- Three types of fibre systems: MEDUSA, IFU, ARGUS (developed at OPM).

- A coordinating observing software, that allows *simultaneous UVES* and *GIRAFFE* observations (developed at ITAL Consortium in collaboration with ESO).

- As for all VLT instruments, a full Data Reduction Software (*DRS*) package is provided, integrated in the ESO Data Flow Software (developed at OGL with contributions from OPM (*GIRAFFE*) and ITAL Consortium (*UVES-Fibre*)).

The FLAMES components are described in detail elsewhere (cf. e.g. Avila et al. 2002, Blecha et al. 2000, Gillingham et al. 2000, 2002, Jocou et al. 2000, Mulas et al. 2002, Pasquini et al. 2000, Royer et al. 2002), on the ESO web site and in the FLAMES User Manual

([www.eso.org/instruments/FLAMES/manuals](http://www.eso.org/instruments/FLAMES/manuals)).

The characteristics of the different observing modes are given in Table 1, which summarizes the observational capabilities of FLAMES.

### UVES-Fibre

UVES is the high-resolution spectrograph of the VLT UT2 (D’Odorico et al. 2000). Each positioner plate has eight fibres connected to the UVES Red Arm. With an aperture on the sky of 1 arcsec, the fibres project to five UVES pixels giving a resolving power of  $\sim 47,000$ . Only the three standard UVES Red set-ups are offered, with central wavelengths of 520, 580 and 860 nm, respectively.

### GIRAFFE

GIRAFFE is a medium-high resolution spectrograph ( $R = 6000\text{--}33,000$ ) for the entire visible range (370–950 nm). It is equipped with two echelles for low and high resolution and uses interference order sorting filters to select the required spectral range within an order. The typical spectral coverage in one exposure is 60–100 nm in low resolution and 20–40 nm in high resolution.

The fibre system feeding GIRAFFE consists of the following components (cf. Avila et al. 2002 for details):

- *MEDUSA* fibre slits, one per positioner plate. Up to 132 separate objects (including sky fibres) are accessible in MEDUSA single fibre mode, each with an aperture of 1.2 arcsec on the sky.

- *IFU* slits. 15 deployable Integral Field Units (IFU) per plate, each consisting of an array of 20 square micro-lenses, for a total (almost rectangular) aperture of  $\sim 3 \times 2$  arcsec. For each plate there are also 15 IFU dedicated to sky measurements.

- *1 ARGUS* slit. A large integral unit consisting of a rectangular array of 22 by 14 micro-lenses, fixed at the centre of one positioner plate. Two scales are available: one with a sampling of 0.52 arcsec/micro-lens and a total aperture of 12 by 7 arcsec, and one with a sam-

pling of 0.3 arcsec/micro-lens and a total coverage of 6.6 by 4.2 arcsec. 15 deployable ARGUS single sky fibres are also available.

GIRAFFE is operated with 30 fixed set-ups (22 high-resolution + 8 low-resolution modes). For performance estimates (based on expected transmission curves and performances) the user is referred to the Exposure Time Calculator (ETC), available at the ESO ETC web page: [www.eso.org/observing/etc](http://www.eso.org/observing/etc)

The FLAMES observing software (OS) is coordinating the operations of the Telescope, the Positioner and the UVES and GIRAFFE spectrographs. In addition, it allows COMBINED observations: that is the simultaneous acquisition of UVES and GIRAFFE spectra with the specific observing modes listed in Table 1.

## LAYOUT

Figure 1 shows a view of the main components of the FLAMES facility, the fibre Positioner and GIRAFFE, as seen on the telescope platform. The Corrector support is also visible, attached at the Nasmyth rotator.

### 1. Corrector

The optical corrector is a big doublet of 880 mm free aperture. The function of the corrector is to give an excellent image quality over the whole 25 arcmin FLAMES field of view and to provide a pupil located at the centre of curvature of the focal plate, to avoid vignetting for off-axis fibres. When the whole optical train is taken into account (including telescope optics and vignetting), the effective transmission of the corrector depends on the observing wavelength and on the distance of the object to the field centre, varying from about 78% at 370 nm to 90% in the visible, and 82% at 1 micron.

A system of lamps has been installed to illuminate the Nasmyth screen, which is located in the telescope centrepiece, about 2 m in front of the focal plane.

## 2. Fibre Positioner (OzPoz)

The Fibre Positioner (OzPoz) is at the core of the FLAMES facility. OzPoz is a rather large and complex system equipped with four plates, two of which are currently in use (cf. Gillingham et al. 2002). The Positioner can be subdivided into the following subsystems:

- Plates: Two metallic disks, on which the magnetic buttons holding the fibres are attached. Each of the plates has a hole in the centre. In one plate this hole hosts ARGUS. Each plate has a curvature of 3950 mm to match the curvature of the corrector focal surface.

- Retractors: Mechanical systems maintaining the fibres in constant tension. Each fibre is equipped with one retractor. The retractors are externally the same for all fibres.

- Exchanger: Main structure holding the plates. The exchanger can perform two main movements: it can retract (or approach) the Nasmyth adapter to engage the plate (or disengage it). Furthermore, it can rotate the upper part in order to perform the plate exchange.

- r- $\theta$  system and Gripper: This unit grips and releases the magnetic buttons at the positions reached via the r- $\theta$  (polar) robot. The gripper requires a back-illumination system, sending a brief light flash along each fibre from the spectrograph towards the plate. A camera records this back-illumination light and performs an image analysis. The back-illumination light is used for several purposes: to reach the required positioning accuracy and to detect if the magnetic button was properly lifted from the plate.

- OzPoz is equipped with a calibration box which can direct the light either from a tungsten, or from a Th-Ar, or from a Ne lamp. In this way FF, Th-Ar and Ne calibrations can be obtained for GIRAFFE and for UVES.

- Field Acquisition Bundles (FACBs): Four magnetic buttons on each plate are equipped with a system of 19 coherent fibres each. This bundle is used to obtain images of fiducial stars, one per button. The four images are viewed by an ESO technical CCD; the image centroids are computed and the proper offsets are calculated to centre the fiducial stars into the bundles. Each FACB bundle has an effective diameter of 2.4 arcseconds.

- Positioning Software: It is written around the so-called delta-task program, developed initially for the 2dF system at AAO. This program allows crossing between the fibres and it determines the button movements sequence.

## 3. Buttons and Fibre Systems

FLAMES is equipped with different types of fibres for UVES and for the dif-

ferent modes for GIRAFFE. It is worth mentioning that, in addition to the object or sky fibres coming from the Positioner, each GIRAFFE fibre slit has five fibres devoted to *simultaneous wavelength calibration*, which provide simultaneous calibration spectra for each observation acquired with GIRAFFE (Hammer et al. 1999).

The histogram distribution of the transmission is given in Figure 2 for the different fibre types. The FLAMES fibres have been proven very robust, so that out of more than 1000 fibres, only a few were broken (and replaced) at the end of the whole process.

### 3.1 UVES fibres

Each of the positioner plates hosts eight 55-metre fibres to guide the light to the UVES spectrograph located on the opposite Nasmyth Platform. From the UVES simultaneous calibration box, one additional 5-metre fibre reaches the UVES-Fibre slit. The fibre centres are separated by 1.7 fibre core, implying that there is some degree of contamination between adjacent fibres; the UVES-Fibre Data Reduction Software (Mulas et al. 2002) has been developed to obtain a complete de-blending of the spectra.

### 3.2 MEDUSA fibres

Each plate also hosts 132 MEDUSA fibres. The separation between each of the MEDUSA fibres in a sub-slit is  $2.26 \times$  the fibre core; this ensures a fibre-to-fibre contamination below 0.5 per cent.

During our tests we have experienced some (about 2%) increased stray light due to reflections from the filter and the (polished) exit slit. We will attempt to reduce this with a stray light mask that reduces the width of the reflecting exit slit viewed from the side of the filter.

### 3.3 IFU fibres

Each Integral Field Unit (IFU) button is composed of twenty micro-lenses arranged in a rectangular shape. The micro-lenses are  $0.52''$  squares. The movable IFUs are a unique characteristic of GIRAFFE and can be placed all over the FLAMES field of view, with the exception of a small fraction of the centre annulus. Each plate hosts fifteen IFUs plus fifteen Sky IFUs. The separation between the fibres' centre is only

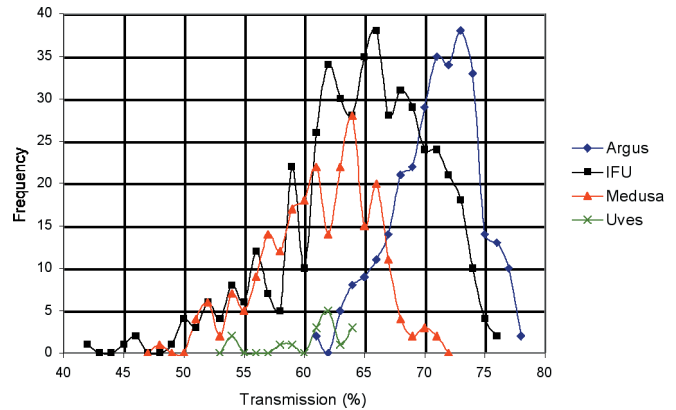


Figure 2: Transmission distribution of all GIRAFFE fibres, as measured in the laboratory.

1.47 times the fibre diameter core, which implies that the contamination between adjacent fibres is about 10 per cent. With the chosen arrangement of the fibres this is acceptable since in normal seeing conditions a higher level of contamination will be present at the fibre entrance level.

### 3.4 ARGUS fibres

The ARGUS system is a fixed array of  $14 \times 22$  micro-lenses, similar to the IFUs, located in the middle of Plate 2. ARGUS is also equipped with a lens to switch between a scale of  $0.52''/\text{micro-lens}$  to a finer scale of  $0.3''/\text{pixel}$ . An ADC ensures that the object images at different wavelengths are maintained in the same locations up to a Zenithal distance of 60 degrees. In addition to the object fibres, fifteen ARGUS sky fibres are present on the plate.

## 4. GIRAFFE

GIRAFFE is a fully dioptic spectrograph. The fibres are arranged in 5 long slits (IFU 1/2, MEDUSA 1/2, ARGUS) at the curved focal plane of the collimator. One of these fibre slits is placed in the working position by a translation stage. The other slits are masked. After leaving the fibres at F/5, the light first passes through one order sorting filter be-

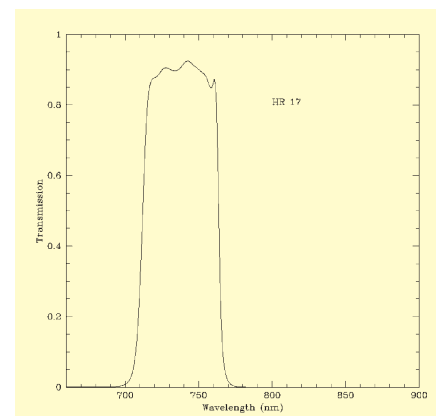


Figure 3: Transmission of order sorting filter HR 17.

Table 2. Summary of GIRAFFE construction characteristics.

Fibre slit height	76.8 mm
Type	Echelle + Order selection Filters
Collimator aperture	F/5
Collimator beam	18 cm
H-R Echelle	204 × 408 mm, 316 lines/mm, 63.4° Blaze
L-R Echelle	156 × 204 mm, 600 lines/mm, 33.7° Blaze
Reimager demagnification ratio	2.5
Effective Camera Focal Length	360 mm
Detector	2048 × 4096, 15 μm EEV CCD
Scale	0.20 arcsec/pixel

fore it is directed to the collimator by a 45-degree mirror. The collimated beam is dispersed by one of the two echelle gratings that are mounted back to back on the grating turret. After passing through the collimator again an intermediate spectrum is produced. Finally, a re-imaging system (“camera”) produces a 2.5 times demagnified image on the 2K × 4K CCD at F/2. A view of GIRAFFE is given in Figure 1. GIRAFFE has been conceived to minimize maintenance and night calibrations; special requirements have been introduced to reduce set-up shifts and to obtain accurate re-positioning, to be able to use wavelength calibrations and flats obtained in the afternoon. To be able to monitor instrument drifts, five fibres are always used to obtain simultaneous calibration spectra.

A summary of the most relevant GIRAFFE characteristics is given in Table 2

GIRAFFE is operated with 30 fixed set-ups; 22 are used to cover the whole spectral range with the high resolution grating, 8 with the low resolution grating. The different GIRAFFE sub-units are described in more detail in the following sections.

#### 4.1 Slit Unit

The slit unit is the most complex GIRAFFE mechanical subsystem, because it needs a very high stability and reproducibility. It has two linear movements: one to exchange the fibre slit, the other one is used for focusing and to press the non-used slits against a baffle that is also used for back-illumi-

nation. The slit unit is equipped with a number of back-illumination LEDs, which are switched on before pick-up and after placing a fibre, to allow the gripper camera to view the fibre output.

#### 4.2 Filters

After the fibre slit, an order-sorting interference filter is placed in the beam. These filters must have excellent transmission and steep bandpass edges and out-of-band blocking, in order to avoid pollution from adjacent spectral orders. One example of filter transmission is given in Figure 3. The transmissions of all filters, averaged over each set-up, are given in Figure 4. This figure shows also the efficiencies of other GIRAFFE components, as well as the overall GIRAFFE efficiency.

#### 4.3 Optics and gratings

The gratings are placed back to back on a turntable. The high-dispersion grating is a MgF<sub>2</sub>/Ag coated, 204 × 408 mm 63.6 degree echelle with a large groove density (316 lines/mm). The 370–950 nm spectral range is covered by twenty-two set-ups in grating orders 15 to 6. Silver was selected because of its good VIS/NIR efficiency and the low polarization it produces on this grating. While the efficiency on one edge of the grating is good through the used spectrum, the efficiency degrades below 500 nm as one approaches the other edge. This is due to inhomogeneity in the MgF<sub>2</sub> layer. We are working to find a replacement up to specifications.

The low-resolution grating has 600

lines/mm coated with MgF<sub>2</sub>/Al. Its first-order blaze lies at 1.96 μm, so in the range 370–950 nm it works in orders 5–2; eight set-ups are needed to cover the full range. After being dispersed, the light passes again through the collimator, forms a real image at an intermediate focal plane and is finally imaged by an F/2 reimaging camera with 7 elements.

#### 4.4 Spectral Format and Efficiency

In GIRAFFE the spectra are parallel in dispersion along the long side of the detector (readout direction), while the short side is along the slit direction. Spectra are slightly curved due to optical distortion and lateral chromatism, with the central part closer to each other than the edges. As is the case in any long-slit spectrograph, the lines of constant wavelength are arranged on low-curvature arcs. An example of a Th-A spectrum taken with MEDUSA is given in Figure 5.

The resolving power and coverage are both a function of the grating angle and grating order: two or three different grating angles are required to fully cover a grating order, which causes the differences in resolution and spectral coverage between the different set-ups. The higher resolving power of the IFU and ARGUS modes (compared to the MEDUSA mode) is due to the smaller size of the fibres, which projects to ~2.2 pixels instead of ~4.3 pixels of MEDUSA, but the spectral coverage for a given set-up is the same in the MEDUSA, IFU and ARGUS modes.

### 5. Integration and Commissioning Results

FLAMES components were installed between October 2001 and April 2002 on UT2. The integration sequence has roughly followed the light path: Corrector, UVES fibres, Positioner, GIRAFFE. GIRAFFE had first light in Europe in December 2001 and was re-assembled in Paranal in April 2002 without major inconveniences, after the re-integration of the positioner and in perfect timing with the rest of the project.

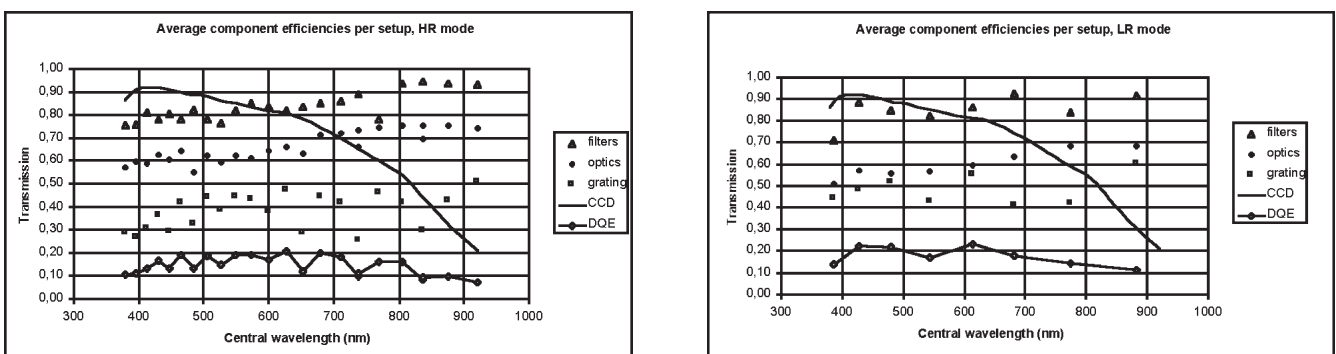


Figure 4: Component efficiencies per set-up and the resulting overall DQE (slit to detected photoelectrons) of GIRAFFE. All reported values are averages; note that grating efficiencies can vary by up to a factor of two within a set-up. The optics efficiency includes vignetting at the grating, this is why the reported LR values are slightly lower than HR values at the same wavelengths.

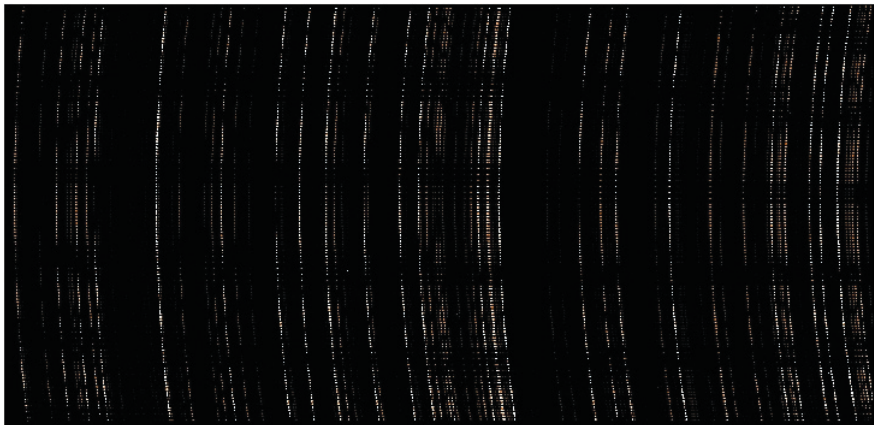


Figure 5: Th-A spectrum taken with a MEDUSA slit. The fibres in the centre of the slit have lines moved towards smaller pixels; e.g. fibres corresponding to the central fibres have slightly redder wavelength coverage than the ones at the CCD edges.

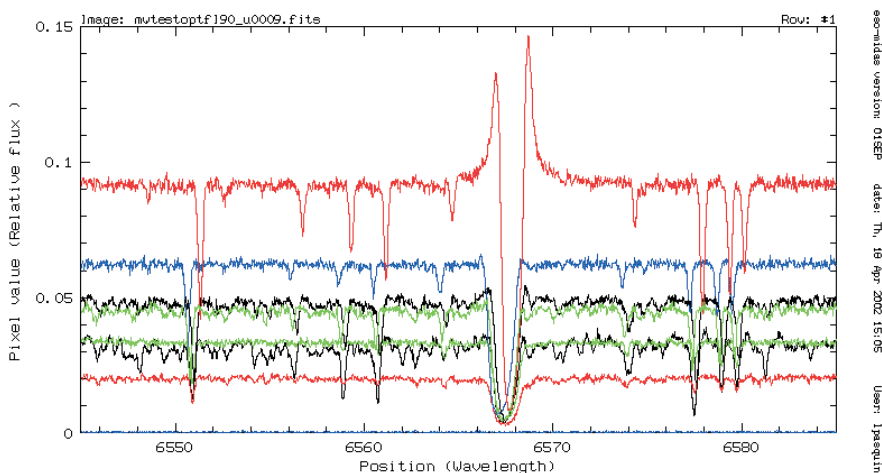


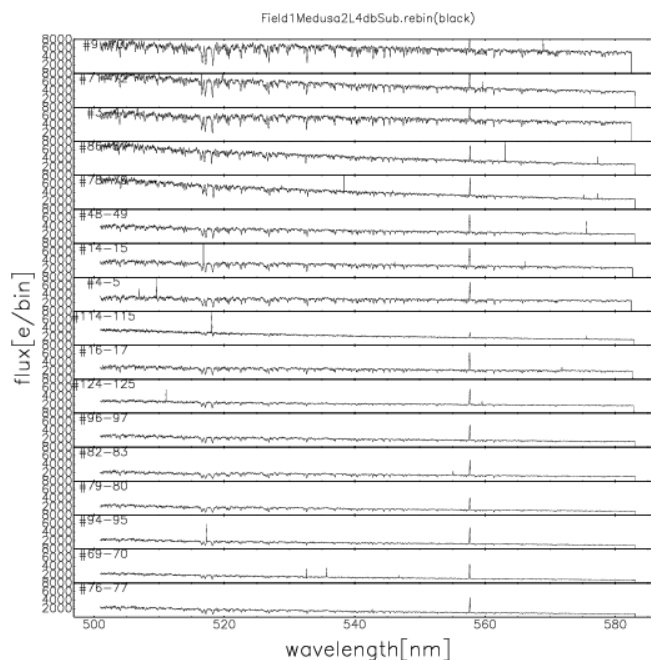
Figure 6: Reduced spectra of 7 giants in the globular cluster Omega Cen taken with UVES-fibre around the H $\alpha$  line.

During the first run at the end of March 2002 the Positioner was integrated and tested and we could gather the first light with UVES-Fibres. Three 10-minute spectra were obtained for 7 stars (one fibre was dedicated to sky) belonging to the Globular cluster Omega Cen. Three of them were previously observed with UVES in long slit mode (Pancino et al. 2002). A small portion of the spectra around the line H $\alpha$  line is shown in Figure 6. The stars had magnitude varying between V = 11.5 and 12.9. After data reduction the equivalent widths of a few hundred lines were compared for the UVES – Fibre and UVES-long slit spectra of the same star, finding an excellent agreement: EQW(Fibre) = EQW(Slit) + A with A in the range of 4–6 mÅ, with an rms of 4–7 mÅ, which is largely due to equivalent widths measurement uncertainties.

During this March run, malfunctions were experienced in the positioner robot, due to the lower temperature at the telescope compared to those prevailing during the tests in Australia and in the Assembly Hall in Paranal. We temporarily fixed this using three heaters,

clearly not a suitable permanent solution. This was corrected prior to a second commissioning period in June but new mechanical problems, related to the interface with the telescope rotator-

Figure 7: Reduced spectra of GIRAFFE from the first commissioning run: the stars belong to an astrometric field. The Mg triplet and the 557 nm sky emission line are clearly visible in all spectra.



adapter were encountered. These problems were cured in advance of the August commissioning run. On July 3, first GIRAFFE spectra could be obtained. Two sets of spectra of stars in an astrometric field were acquired, each of 10 minutes. The set-up used was LR4, Low Resolution centred at a wavelength close to the V filter. 66 MEDUSA fibres were positioned (some in sky positions), and the reduced spectra of some of them are shown in Figure 7. The stars have R magnitudes between 13 and 14. In all spectra the Magnesium triplet at 518 nm is clearly visible, as well as the 557 sky emission line.

The stability and repeatability of GIRAFFE on the telescope, measured by taking a ThAr spectrum every 4 hours over a period of 2 weeks is shown in Figures 8 and 9.

The tests have been very satisfactory, showing that the instrument exceeds specifications.

A further commissioning took place in August 2002, enabling us to advance the commissioning tests. Many MEDUSA ‘rasters’ have been performed, to determine the telescope-plate geometry.

In these rasters an astrometric field is observed with MEDUSA and the telescope is offset along a grid around the pointing position. For every star, the distance between its nominal position (the centre of the grid) and the positions of its maximum flux is then computed and used to correct the astrometric model. The results have been so far very encouraging, and the found residuals are shown in Figure 10, with an RMS of 0.15 arcseconds, which is very good when considering that this number includes all sources of errors, e.g., the accuracy of the stellar astrometry. In Figure 11 we show the image of 4

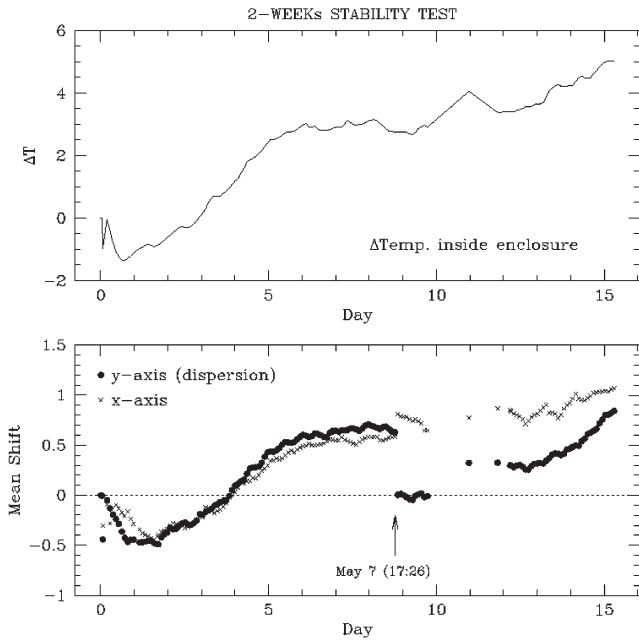
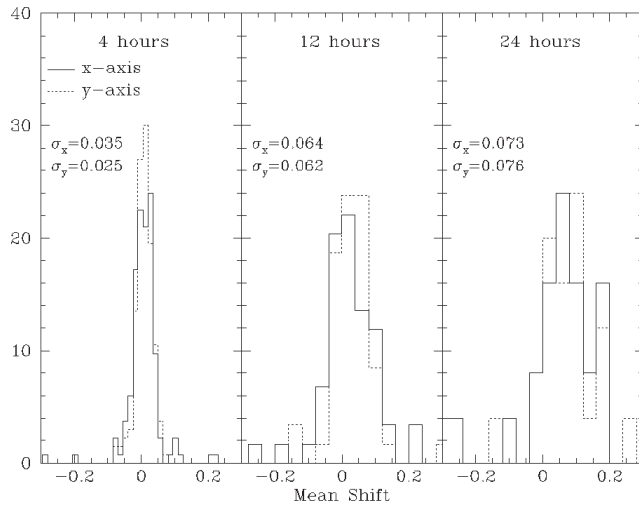


Figure 8: the average position of ThAr lines in a time series that was taken at 4-h intervals over a period of 2 weeks. Shifts are given in pixels relative to the first exposure. These exposures were taken in Medusa HR mode, with configuration changes between exposures. The jump on May 7 cannot be correlated to any known event like an earthquake.



▲ Figure 9: Histogram of relative shifts after 4, 12 and 24 hours, using the time series of Figure 12. In HR mode, 0.1 pixel corresponds to about 300 m/sec. These plots show the intrinsic stability of Giraffe and will be helpful to plan the frequency of calibrations. Note that we expect to obtain higher radial velocity precision by using the simultaneous calibration fibres.

stars from the Tycho catalogue well centred in the FACBs after the telescope field acquisition has been completed.

Two recurrent questions when using fibres are the capability of obtaining good flat field corrections, and to subtract the sky. Sky subtraction tests are under way, while flat field correction capabilities have been evaluated. In Figure 12 is shown the comparison between the measured S/N ratio in a por-

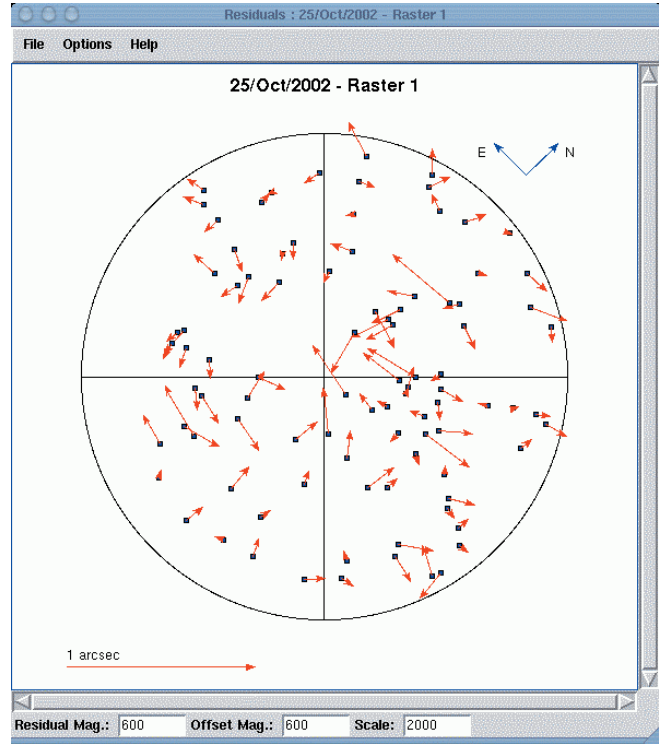


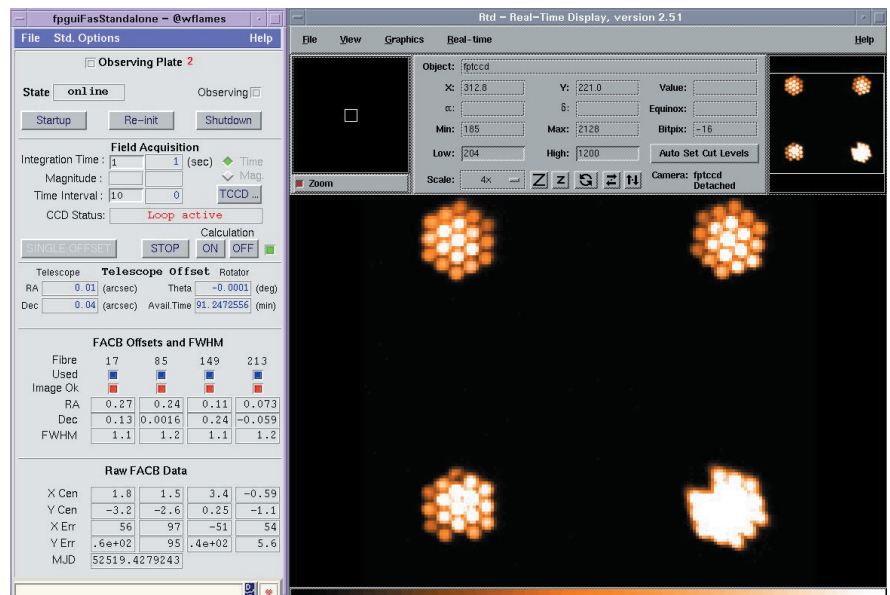
Figure 10: Residuals vectors after the subtraction of the position centroid from the object fibre, after a successful modelling of the plate geometry.

tion of the spectra of several stars in the SMC, acquired with the L8 set-up, a spectral range plagued by strong fringing. We searched for a 'line free' region in the spectra and the S/N ratio has been computed in this small (typically less than 2 nm) spectral region. In ordinate the Poisson noise

based on the number of detected electrons is given. The agreement between the measured and Poisson S/N ratio is quite good.

In the past, several groups have reported problems in obtaining accurate

Figure 11: After a successful acquisition is completed, the four fiducial stars should be well centred in the FACBs, as in the case of these 4 stars from the Tycho Catalogue. The observations were made at airmass 1.8 which shows the good handling of atmospheric effects by the positioner SW. The figure shows the Graphic User Interface at the UT2 Console.



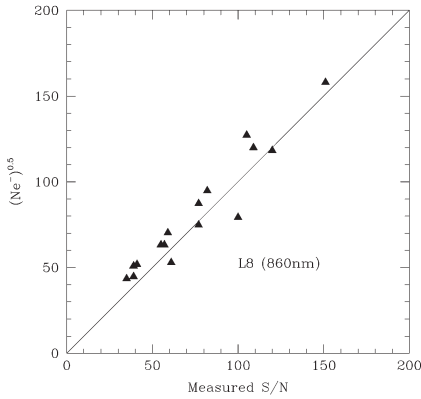


Figure 12: S/N ratio as measured in clean regions of spectra taken in the L8 set-up, compared with the Poisson S/N ratio expected on the number of counts recorded.

flat fielding while using fibres, because, if spatial filters are present in the optical path, variable fringing pattern can be produced in the spectra.

By dividing 3 FF taken with the fibre positioner by the mean of 36 FF taken with the Nasmyth screen, a S/N ratio of 400 was obtained. This S/N ratio obtained was less than what expected by Poisson noise statistics, but it shows that this problem is limited in the FLAMES system to very high S/N observations. Note that the 3 positioner FF represent the standard calibrations that the observer will receive. Similarly we have tested the stability of photometric response of the fibres to torsion and movements: by taking Nasmyth FF and after rotating by a full circle, the photometric stability has been shown to be better than 0.5 %. Finally, in order to perform an accurate sky subtraction, the relative fibre transmission needs to be known accurately. By comparing fibre to fibre transmission by using 3 positioner flats (standard calibrations) with that obtained by the average of the 36 Nasmyth flats, we find that the two measurements agree to better than 3% rms. This is a good result, although not yet within the specifications (2%).

We have performed several comparisons with the ESO Exposure Time Calculator (ETC, [www.eso.org/observing/etc](http://www.eso.org/observing/etc)). In Figure 13 we show the results of the comparison between the flux observed vs. the flux predicted as obtained by observing an astrometric field (the astrometric solution in use in this test had a residual rms of 0.24 arcseconds). The Figure shows the number of counts recorded vs. R magnitude, while the curve shows the prediction by the ETC in the L8 set-up for a G0 star and the parameters (seeing, exposure time) appropriate for the observation. As shown in the bottom panel, at any given magnitude, the number of collected  $e^-$  per object is represented by a relatively broad distribution. This is due to several factors, such as the variation in the fibre transmission,

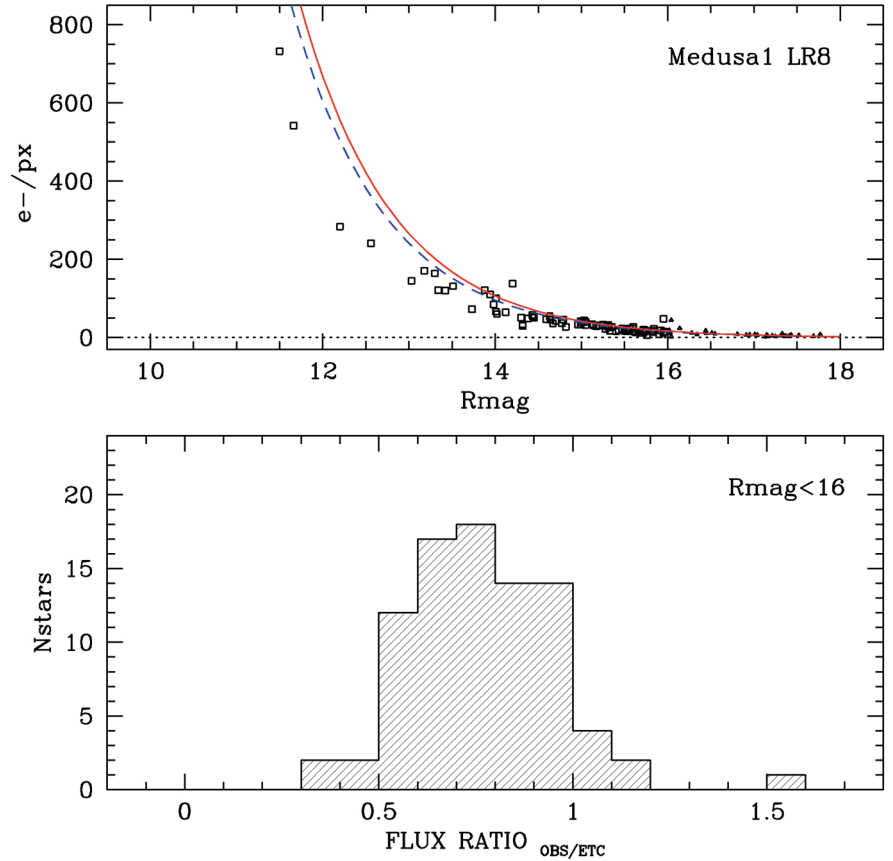


Figure 13: Comparison between observed flux and predicted ETC flux for an astrometric field with the L8 set-up. The histogram shows the ratio measured/expected. The ETC calculations are based on a G0 spectral type.

the poor astrometry of some targets, and the difference in spectral type among the stars in the catalogue. On

the other hand, it is important that the potential users become familiar with the concept that for FLAMES the S/N

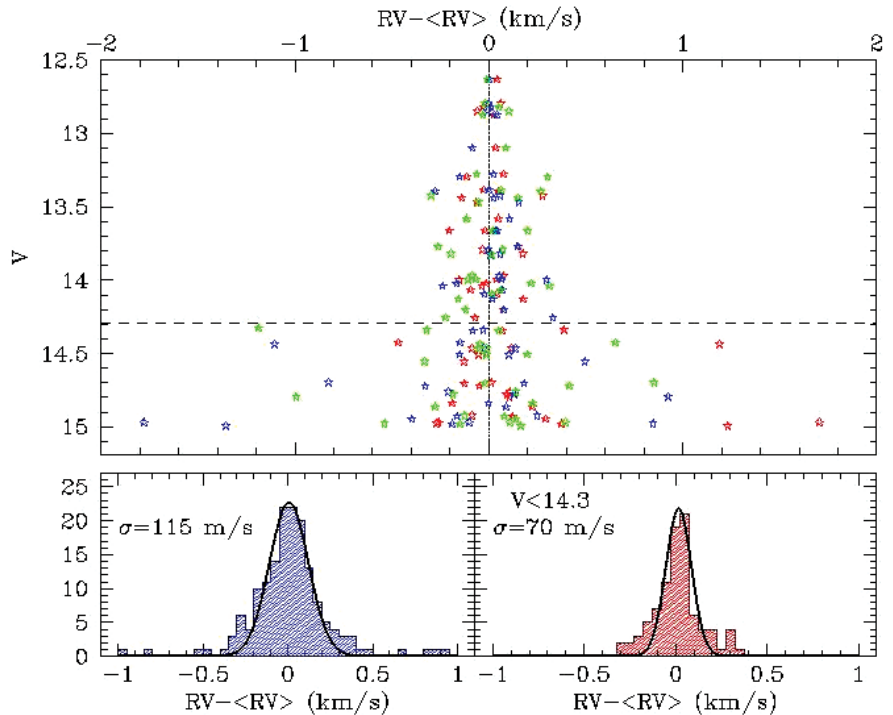


Figure 14: Distribution of the difference between RV single measurements and RV mean for 3 exposures taken in 1 night of 60 stars of the globular cluster NGC 6809, shown vs. the stellar magnitude. Points from the different observations are shown with different colours. In the lower panel, the left distribution refers to all the measurements, irrespective of stellar magnitude. The right distribution includes only the bright ( $V < 14.3$ ) subsample.

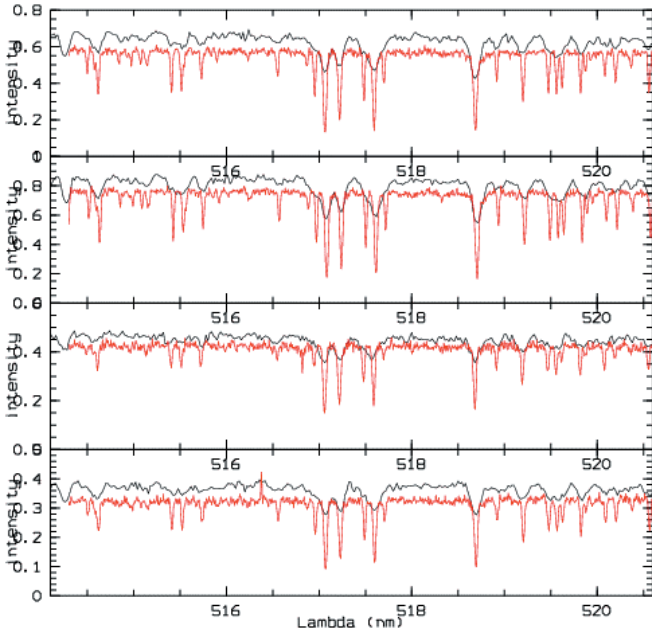


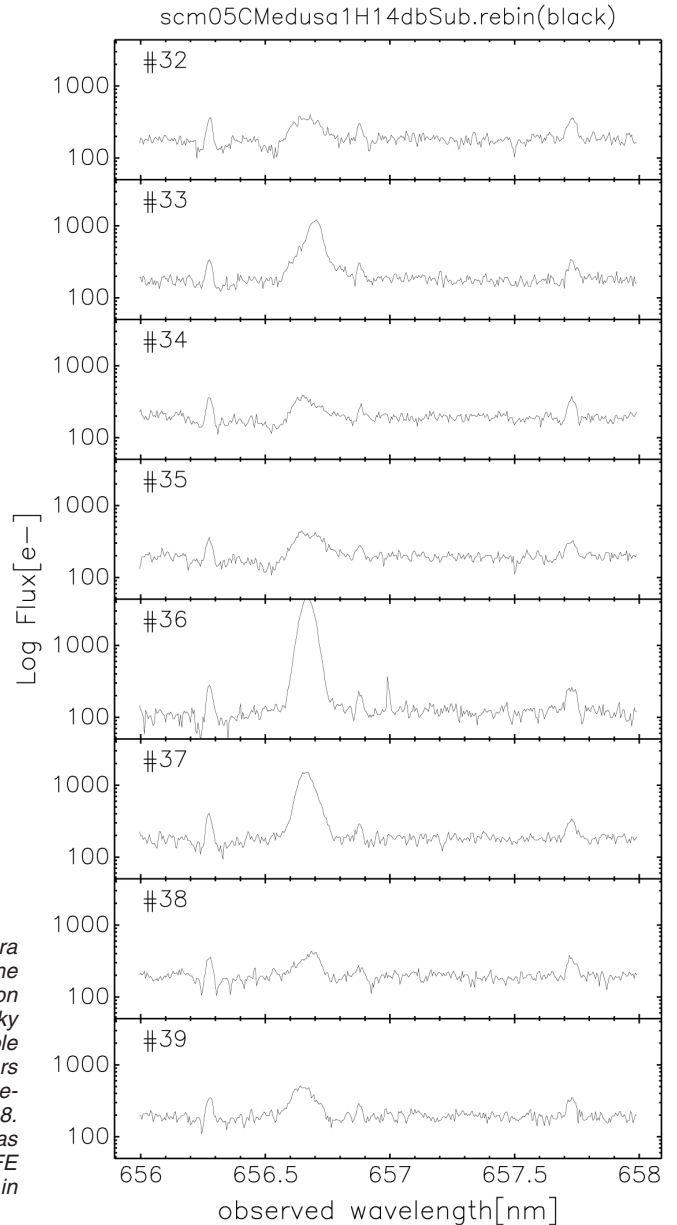
Figure 15: GIRAFFE Low (L4, black lines) and High (H9, red lines) resolution spectra of 4 giants belonging to the Globular Cluster NGC 6809

ratio predicted by the ETC will always have to be intended in a statistical sense.

A number of tests have been performed to characterize the GIRAFFE radial velocity (RV) capabilities, observing the same objects several time in a night, as well as in different nights. Three not consecutive observations of 15 minutes in the GIRAFFE H9 set-up were obtained in the same night for 96 giants at the centre of the Globular Cluster NGC6809. The stars were selected between magnitude 13 and 15 and the observations made with a non optimal astrometric model. Out of the full sample (96 stars) we analysed only 60 objects giving a well determined cross correlation peak.

Out of these 11 were further excluded because their RV were either discordant from the bulk of the cluster, or because they showed a very large RV difference in the 3 measurements (4 stars). Based on the 3 measurements of the 49 stars left, the cluster velocity is found at 178.81 km/sec (note that this RV is computed with respect to our digital mask, no attempt has been made to transform it to an absolute RV), with a dispersion of 4.057 km/sec. In Figure 14 the distribution of the differences of all the measurements with respect to their mean values are shown. This figure clearly shows how the Radial Velocity accuracy degrades with increasing stellar magnitude (and therefore decreasing fluxes); the three observation points are indicated with different colours. When taking all the points, irrespective of the stellar magnitudes, the  $\sigma$  of the distribution is of 113 m/sec, while if only the bright end is considered,  $V < 14.3$ , the  $\sigma$  decreases

Figure 16:  $H\alpha$  Spectra of 8 red giants in the SMC, no sky subtraction was performed, and sky  $H\alpha$  in emission is visible at 6562.8 nm. The stars have V magnitude between 18.5 and 18.8. The exposure time was 1 hour, in the GIRAFFE H14 setup. Fluxes are in Log scale.



to 70 m/sec. These numbers are indicative of the accuracy reached in the time scale of a few hours and normal operations. Royer et al. (2002) have reached a short-term accuracy of 13 m/sec with GIRAFFE, in a more stable environment, using much higher S/N observations of the solar light in the Garching Integration Hall.

We had the opportunity to observe the same NGC 6809 field also with GIRAFFE in low resolution mode (L4) and in Figure 15 a fraction of the spectra of the same stars (4 giants belonging to the cluster) observed in L4 and H9 at a resolving power of  $R = 6000$  and  $R = 26,000$  respectively are shown. The integration time in the HR9 was 2 times longer than in the LR4 .

We are acquiring spectra to verify the behaviour of the instruments at the faint end of the magnitude range; Figure 16 shows a collection of  $H\alpha$  spectra taken with the high resolution grating of GIRAFFE (set-up H14) of giants on the

Red Giant Branch of the Small Magellanic Cloud; the magnitudes vary between  $V = 18.5$  and 18.8, the exposure time was of 1 hour with an 0.9 arc-second seeing.

Spectra were acquired for a field of galaxies with the Giraffe IFUs, and their reduction is not yet completed. We aim at making a release of FLAMES commissioning data in the first quarter of 2003.

## 6. Acknowledgements

The development of FLAMES, which was recommended by the ESO STC in 1998, presented some remarkable aspects, showing the feasibility of a complex, multi-institute facility in a short time. This could not have been possible without appropriate structures but mostly without the dedicated work of a very large number of people, whose names do not appear in the author list. We thank all the persons at ESO

(Garching and Paranal) and at the different institutions who have contributed to the realization of this ambitious project: J. Alonso, P. Ballester, J.-L. Beckers, P. Biereichel, B. Buzzoni, C. Cavadore, N. Cretton, C. Cumani, B. Delabre, A.V. Kesteren, H. Kotzlowski, J.-L. Lizon, R.S. Moreau, W. Nees, R. Palsa, E. Pozna, (ESO), P. Barriga, R. Castillo, J. Spyromilio AND MANY OTHERS at Paranal, C. Evans, R. Haynes, U. Klauser, B. Hingley, D. Mayfield, S. Miziarski, R. Muller, W. Saunders, G. Schafer, K. Shortridge, (AAO), L. Jocou and the fibre team, T. Melse and the mechanics workshop team, S. Baratchart, L. Chemin, H. Flores, D. Horville, J.M., Huet, F. Rigaud, F. Sayède (GEPI, OPM), F.R. Ferraro,

P. Molaro, R. Pallavicini, I. Porceddu (ITAL Consortium).

### References

Avila, G. Guinouard, I., Jocou, L., Guillon, F., Balsamo, F. 2002, in *Instrument Design and Performance for Optical/Infrared Ground-Based Telescopes* Proc. SPIE **4841** (in press).  
 Blecha, A., North, P., Cayatte, V., Royer, F., Simond, G. 2000, Proc. SPIE Vol. **4008**, p. 467.  
 D'Odorico, S. et al. 2000, Proc. SPIE Vol. **4005**, p. 121.  
 Gillingham, P., Miziarski, S., Klauser, U. 2000, Proc. SPIE Vol. **4008**, p. 914.  
 Gillingham P.R., Popovic D., Waller L.G., Farrell T.J. 2002, in *Instrument Design and Performance for Optical/Infrared Ground-Based Telescopes*, Proc. SPIE **4841** (in press).

Hammer, F., Hill, V., Cayatte, V. 1999, *Journal des Astronomes Français*, **60**, 19.  
 Jocou, I. et al. 2000, Proc. SPIE Vol. **4008**, p. 475.  
 Mulas, G., Modigliani, A., Porceddu, I., Damiani, F. 2002, in *Instrument Design and Performances for Optical/Infrared Ground-Based Telescopes*, Proc. SPIE **4841** (in press).  
 Pancino, E. et al. 2002: *ApJ* **568**, L101.  
 Pasquini, L. et al. 2000, Proc. SPIE Vol. **4008**, p. 129.  
 Pasquini, L. et al. 2002, in *Instrument Design and Performances for Optical/Infrared Ground-Based Telescopes*, Proc. SPIE **4841** (in press).  
 Royer, F., Blecha, A., North, P., Simond, G., Baratchart, S., Cayatte, V., Chemin, L., Palsa, R. 2002, in *Astronomical Data Analysis II*, Proc SPIE **4847** (in press).

# HARPS: ESO's Coming Planet Searcher

## Chasing Exoplanets with the La Silla 3.6-m Telescope

F. PEPE<sup>1</sup>, M. MAYOR<sup>1</sup>, G. RUPPRECHT<sup>3</sup>

email: Francesco.Pepe@obs.unige.ch; Michel.Mayor@obs.unige.ch; grupprec@eso.org

with the collaboration of the HARPS Team: G. AVILA<sup>3</sup>, P. BALLESTER<sup>3</sup>, J.-L. BECKERS<sup>3</sup>, W. BENZ<sup>5</sup>, J.-L. BERTAUX<sup>6</sup>, F. BOUCHY<sup>1</sup>, B. BUZZONI<sup>3</sup>, C. CAVADORE<sup>3</sup>, S. DEIRIES<sup>3</sup>, H. DEKKER<sup>3</sup>, B. DELABRE<sup>3</sup>, S. D'ODORICO<sup>3</sup>, W. ECKERT<sup>2</sup>, J. FISCHER<sup>5</sup>, M. FLEURY<sup>1</sup>, M. GEORGE<sup>1</sup>, A. GILLIOTTE<sup>2</sup>, D. GOJAK<sup>2,3</sup>, J.-C. GUZMAN<sup>2</sup>, F. KOCH<sup>3</sup>, D. KOHLER<sup>4</sup>, H. KOTZLOWSKI, D. LACROIX<sup>3</sup>, J. LE MERRER<sup>10</sup>, J.-L. LIZON<sup>3</sup>, G. LO CURTO<sup>2</sup>, A. LONGINOTTI<sup>3</sup>, D. MEGEVAND<sup>1</sup>, L. PASQUINI<sup>3</sup>, P. PETITPAS<sup>4</sup>, M. PICHARD<sup>1</sup>, D. QUELOZ<sup>1</sup>, J. REYES<sup>3</sup>, P. RICHAUD<sup>4</sup>, J.-P. SIVAN<sup>4</sup>, D. SOSNOWSKA<sup>1</sup>, R. SOTO<sup>2</sup>, S. UDRY<sup>1</sup>, E. URETA<sup>2</sup>, A. VAN KESTEREN<sup>3</sup>, L. WEBER<sup>1</sup>, U. WEILENMANN<sup>2</sup>, A. WICENEC<sup>3</sup>, G. WIELAND<sup>3</sup> and advice by the Instrument Science Team: J. CHRISTENSEN-DALSGAARD<sup>7</sup>, D. DRAVINS<sup>8</sup>, A. HATZES<sup>9</sup>, M. KÜRSTER<sup>9</sup>, F. PARESCE<sup>3</sup>, A. PENNY<sup>11</sup>

<sup>1</sup>Observatoire de Genève; <sup>2</sup>ESO, La Silla; <sup>3</sup>ESO, Garching; <sup>4</sup>Observatoire de Haute Provence; <sup>5</sup>Physikalisches Institut, Bern; <sup>6</sup>Service d'Aéronomie du CNRS; <sup>7</sup>Aarhus University, <sup>8</sup>Lund Observatory, <sup>9</sup>Tautenburger Landessternwarte; <sup>10</sup>Laboratoire d'Astrophysique de Marseille; <sup>11</sup>Rutherford Appleton Laboratory

### Introduction

An extensive review of past, present and future research on extrasolar planets is given in the article "Extrasolar Planets" by N. Santos et al. in the present issue of *The Messenger*. Here we want to mention only that the search for extrasolar planets and the interpretation of the scientific results have evolved in recent years into one of the most exciting and dynamic research topics in modern astronomy.

As a consequence, ESO decided to have a dedicated spectrograph built to be installed at the La Silla 3.6-m telescope. An Announcement of Opportunity was issued in 1998 and a consortium chosen for the realization of the project which consists of Observatoire de Haute Provence (F), Physikalisches

Institut der Universität Bern (CH) and Service d'Aéronomie du CNRS (F) under the leadership of the Observatoire de Genève (CH) where the Principal Investigator and the Project Office are located. Further contributions come from ESO-La Silla and ESO Headquarters (Garching). The agreement was finally signed in August 2000.

According to this agreement, the HARPS Consortium bears the cost for the spectrograph and all its components whereas ESO provides the Cassegrain Fibre Adapter, the fibre link, the dedicated HARPS room in the telescope building and the complete detector system. In return, the HARPS Consortium will be granted 100 HARPS observing nights per year for a period of 5 years after successful Provisional Acceptance in Chile. HARPS will of

course also be offered to the astronomical community like any other ESO instrument.

### The Radial Velocity Method: Error Sources

A description of the radial velocity method for the detection of extrasolar planets in general and of the CORALIE spectrograph installed at the Swiss Leonhard Euler Telescope at La Silla in particular was given by Queloz & Mayor (2001); it describes the technique applied also with HARPS and the spectrograph which is its direct ancestor. An instrument like CORALIE achieves an accuracy in radial velocity determination of about 3 m/s, and with this accuracy planets down to a minimum mass of about one third the mass of Saturn